Thermomechanics of mid-ocean ridge segmentation

Eun-seo Choi[1], Luc Lavier[2], Michael Gurnis[1]

[1]Seismological Laboratory, California Institute of Technology, Pasadena, CA 91125, U.S.A.

[2]Institute of Geophysics, University of Texas, Austin

ces74@gps.caltech.edu

Abstract

The mechanics responsible for the initiation of the orthogonal pattern characterizing mid-ocean ridges and transform faults are studied using numerical models. The driving forces are thermal stresses arising from the cooling of young oceanic crust and extensional kinematic boundary conditions. Thermal stress can exert ridge-parallel tension comparable to spreading-induced stress when selectively released by ridges and ridge-parallel structure. Two modes of ridge segment growth have been identified in plan view: An overlapping mode where ridge segments overlap and bend toward each other and a connecting mode where two ridge segments are connected by a transform-like fault. As the ratio of thermal stress to spreading-induced stress (γ) increases, the patterns of localized plastic strain on the top surface change from the overlapping to connecting mode. The orthogonal pattern marks the transition from one mode to the other. Besides the amount of stress from each driving force, the rate of stress accumulation is crucial in determining the emergent pattern. This rate-dependence is characterized by the spreading rate normalized by a reference-cooling rate (Pe'). When Pe' is paired with the ratio of thermal stress to spreading-induced stresses (γ'), they define stability fields of the two modes. The obliquely connecting, the orthogonally connecting, and the overlapping mode are similar to the ridge-transform fault intersection observed in ultraslow, slow to intermediate, and fast spreading centers, respectively. The patterns are also sensitive to the strain weakening rate. Fracture zones were created in part as a response to thermal stress.

Introduction

A plausible source for ridge-parallel tension is the cooling of oceanic lithosphere. Thermal cooling stresses make a significant contribution to the stress state of oceanic plates. Thermal stresses are isotropic, but mid-ocean ridges themselves and numerous ridge parallel faults can release thermal stresses in a selective (i.e., ridge-perpendicular) direction when these structures form (Fig. 1). Therefore, the resultant unreleased stress due to cooling would be dominated by the ridge-parallel component.

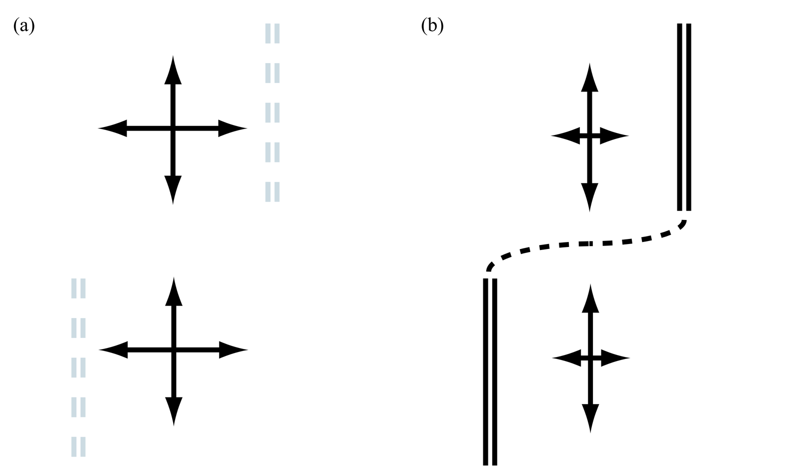

FIGURE 1: Arrows represent the direction and magnitude of principal components of thermal stresses along ridge-perpendicular and ridge-parallel directions. (a) Before ridge segments are created, thermal stress is isotropic and its horizontal components are equal in magnitude. The future location of ridge segments are marked by the pairs of gray dashed lines. (b) The ridge-parallel component becomes dominant when the ridge-normal principal stress is released by the formation of ridge segments (pairs of solid lines). A possible trace of a structure connecting the ridge segments is denoted by a dased curve.

The role of thermal stress was important in analog experiments. Oldenburg and Brune [JGR, 1972] designed an experiment in which the surface of molten wax was chilled by a fan. They observed the spontaneous growth of an orthogonal system of ridge, transform faults, and fracture zones with characteristics similar to natural systems.

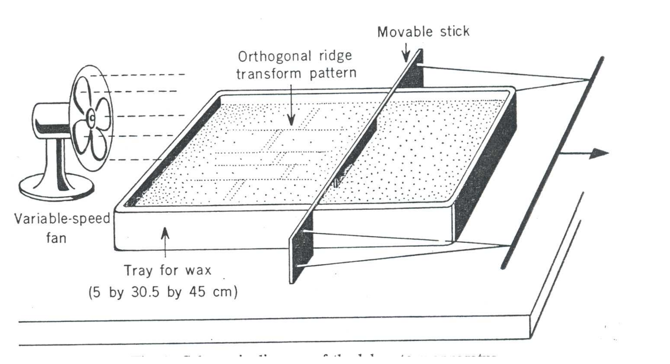

FIGURE 2: Apparatus setup for the wax experiment by Oldenburg and Brune [1972].

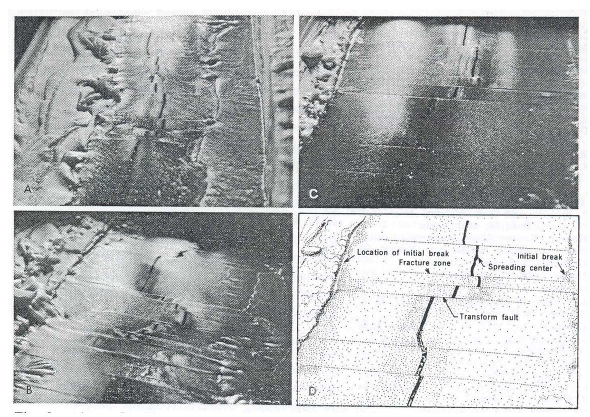

FIGURE 3: Patterns formed on the frozen surface of wax [Oldenburg and Brune, 1972].

Numerical Method

We turn to a numerical approach although wax models' success in creating the patterns appears to imply that the patterns are made by the very mechanism acting along mid-ocean ridge. Using numerical simulations, known representative values for the Earth's material can be directly used in models. In addition, numerical experiments allow for a better control on testable mechanisms and a wide range of parameter values. Numerical models can also be used to make explicit predictions of geophysical observations such as bathymetry and gravity.

We use SNAC (**S**tGermai**N** **A**nalysis of **C**ontinua), which is an energy-based finite difference code solving equations of momentum balance and heat energy conservation. SNAC can descritize a fully 3-D model domain into a structured tetrahedral mesh. Lagrangian description of motion is adopted. The following features of SNAC are noteworthy:

Mixed Discretization: To deal with incompressibility, volumetric strain in individual tetrahedron is replaced with an average over two overlays (see Fig. 4).

Remeshing: Lagrangian meshes are remeshed to relieve extreme mesh distortion. Nodal values are interpolated from the old mesh to the new one; element values are transferred between the nearest neighbors (Fig. 5).

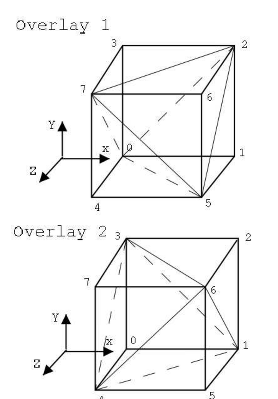

FIGURE 4: Two different discretizations of a cube with tetrahedra are used for computing average volumetric strain and for symmetric response.

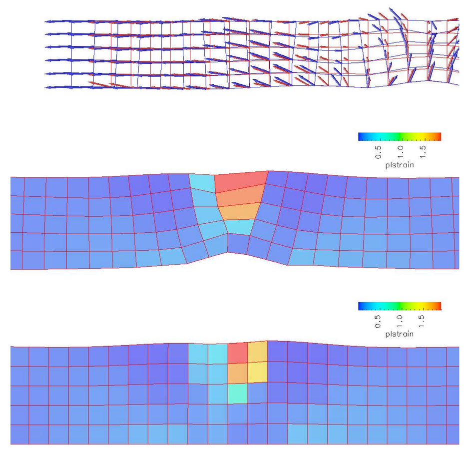

FIGURE 5: **Top**: Velocity, a node-associated field, is interpolated from the old (blue) to the new (red) mesh. **Middle**: The distribution of plastic strain, an element-associated field, is shown with a deformed mesh. **Bottom**: The plastic strain field has been transferred between the nearest neighbor tetrahedra during remeshing.

Constitutive Model: Total strain is assumed to be the sum of ealstic, viscous, and plastic strain. This consititutive model assumes Maxwell viscoelasticity as a base rheology. When stress increases faster than the relaxation rate, material can yield according to a given criterion: *e.g.*, the Mohr-Coulomb model. Viscosity can be Newtonian or a power-law type.

Model Setup

A hot block of oceanic crust cools while it is stretched at a given spreading rate. Spreading initiates ridge segments, which in turn releases accumulating thermal stress only in the ridge-normal direction. Initial temperature is uniformly 1300 $°C$ except along the top surface, where temperature is 0 $°C$. The top surface remains isothermal at 0 $°C$, while the bottom surface has a zero heat flux. These thermal initial and boundary conditions are intended to be those of hypothetically pristine oceanic crust that is about to cool and extend.

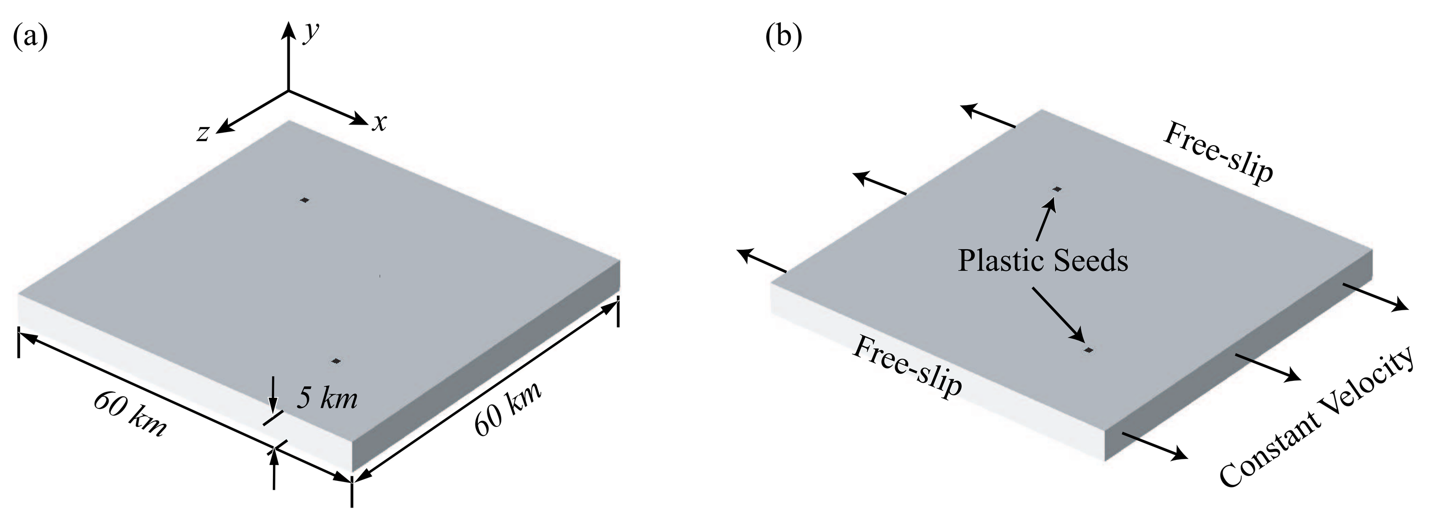

FIGURE 6: Geometry of the model domain. (a) 60 km × 5 km × 60 km domain with equal 1 km grid spacing in each direction. (b) Two side surfaces normal to the x axis are pulled at a constant velocity. The other two sides, normal to z axis, have free-slip boundary conditions. The bottom is supported by a Winkler foundation. Two plastic seeds, controlling initial localization, are embedded with 30 km separation in the x and z directions.

Results

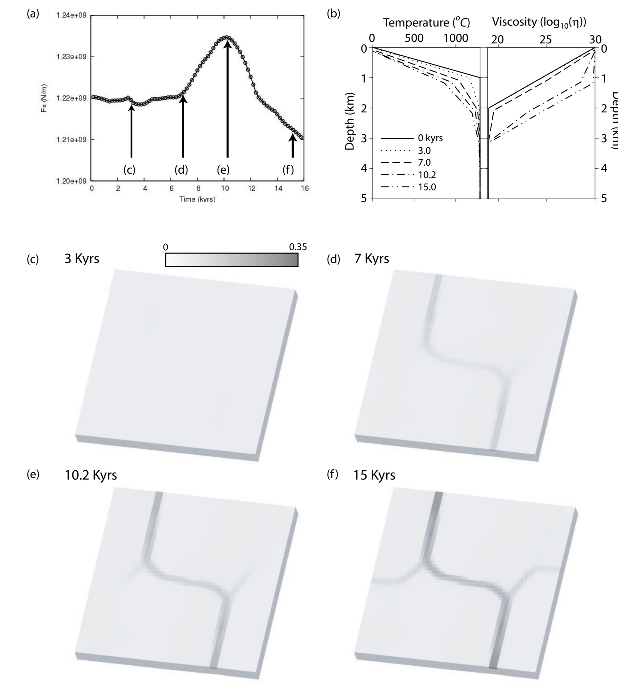

FIGURE 7: (a) Fx, force required to extend the domain at the applied velocity in the x-direction as a function of time. (b) Depth profiles of temperature and viscosity are compared at different time steps (0, 3, 7, 10.2, and 15 Kyrs). The rise in Fx at approx. 7 Kyrs coincides with the cooling and significant increase in viscosity of the subsurface (1-2 km deep) layer. 3-D rendering of the second invariant of plastic strain at the same set of time steps: (c) 3 Kyrs, (d) 7 Kyrs, (e) 10.2 Kyrs, and (f) 15 Kyrs.

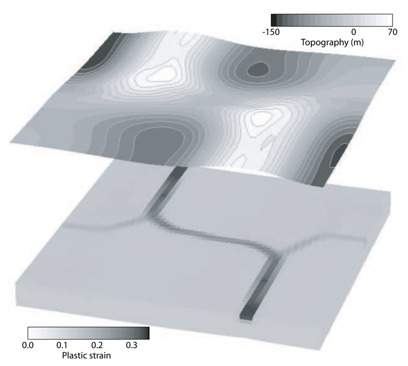

FIGURE 8: A 3-D representation of the surface topography from the base model at 15 Kyrs on top of the model domain. Plastic strain on the surface of the model domain indicated through grey scale shading.

To assess quantitatively the relative influence of thermal stress to spreading-induced stress on the appearance of localization patterns, we introduce a dimensionless number γ. γ is defined as the ratio of the first invariant of thermal stress to the first invariant of spreading-induced stress. Since the domain geometry (D and L) and the temperature initial condition (ΔT) are common to all the models, we vary the remaining three parameters, v, α_v, and κ to determine their influence on the pattern of localization.

Definitions

$$\gamma = |I_\sigma^{therm}|/|I_\sigma^{spr}|$$
$$I_\sigma^{therm} = -(3\lambda + 2\mu)\alpha_V(T - T_0)$$
$$I_\sigma^{spr} = (3\lambda + 2\mu)\varepsilon_{11}^{spr}$$
$$\therefore \gamma = \frac{(3\lambda + 2\mu)\alpha_V(T - T_0)}{(3\lambda + 2\mu)\varepsilon_{11}^{spr}}$$
$$= \frac{\alpha_V(\kappa\nabla^2 T)\Delta t}{\dot{\varepsilon}_\sigma^{spr}\Delta t} = \frac{\alpha_V(\kappa\Delta T/D^2)}{v/L}$$
$$= \frac{\alpha_V(\kappa\Delta T)L}{vD^2}$$
$$\gamma' = \frac{\alpha_V(\kappa\Delta T)L}{v_{ref}D^2}, \text{ and } Pe' = \frac{vD}{\kappa_{ref}}$$

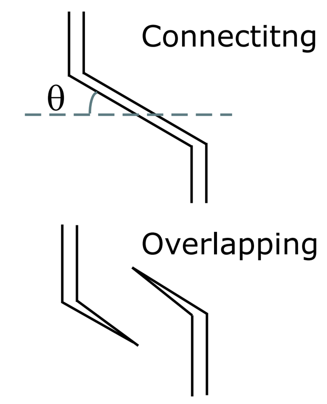

FIGURE 9: Modes of interaction between two mutually approaching ridge segments. The orthogonal ridge transform fault geometry is a special case of the "connecting mode". The angle, θ, is used as a measure of a connecting pattern's orthogonality spanning the range 0° to 45°.

Those models with the same γ but different parameters can produce considerably different patterns because the growth rates of stresses from cooling and spreading are different even for the proportionally varied parameters. So, we use the Peclet number as another measure of the system which we physically interprete here as the ratio of forced spreading rate (v) to cooling rate (κ/D). To ensure that separate measures of each process are not inherently correlated by sharing common parameters, we compute them with respect to reference values of v and κ/D.

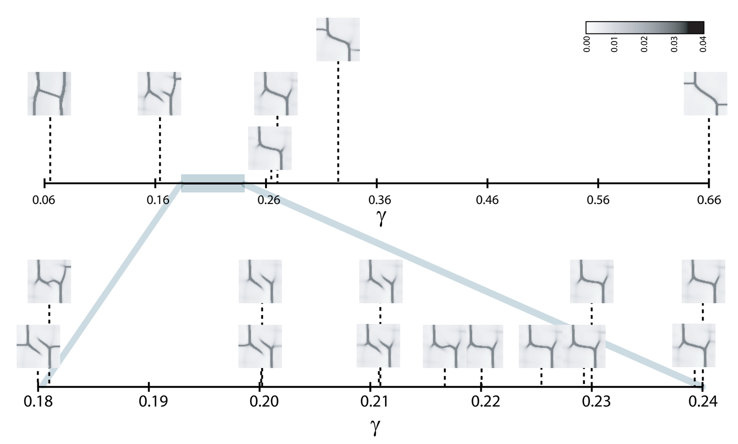

FIGURE 10: Patterns of localized plastic strain, made on the top surface of models, are arranged in order of increasing γ. The patterns were captured after 10.6 kyrs. As γ increases, the mode of interaction between two mutually-approaching ridge segments changes from overlapping through orthogonal rifting to oblique rifting.

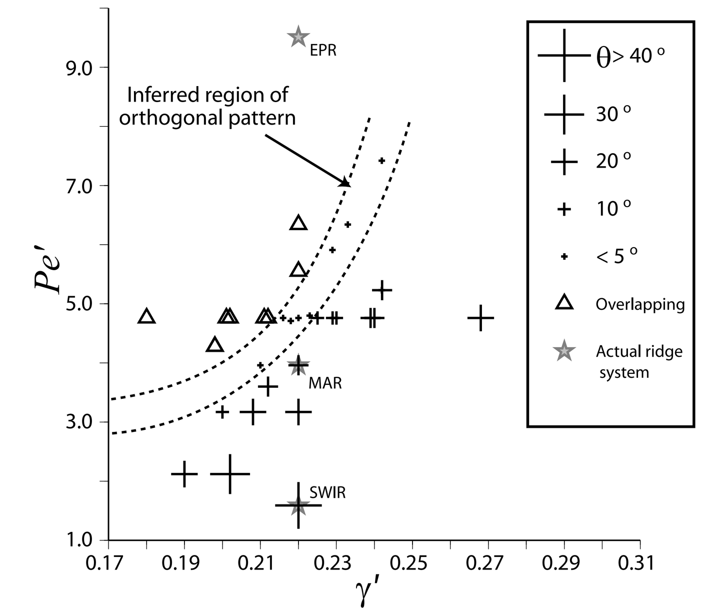

FIGURE 11: Plot of Pe' versus γ'. The domain of connecting and overlapping mode is well defined and the boundary between them defines the stability field of the orthogonal pattern. Within the connecting-mode domain, the variation in θ is systematic: θ becomes smaller as the values of Pe'-γ' pair gets closer to the inferred region of orthogonal pattern.